Fluctuation pressure of a membrane between walls through five loops

Boris Kastening*
Institut für Theoretische Physik, Freie Universität Berlin, Arnimallee 14, D-14195 Berlin, Germany
(Received 7 May 2002; published 16 December 2002)

An earlier four-loop calculation of the fluctuation pressure of a fluid membrane between two infinite walls is extended to five loops. Variational perturbation theory is used to extract the hard-wall limit from perturbative results obtained with a smooth potential. Comparison with a structurally similar quantum mechanics problem of a particle in a box is used for an alternative way of extracting the membrane pressure and also to estimate the quality of the results. Our values lie above the best available Monte Carlo data.

DOI: 10.1103/PhysRevE.66.061102 PACS number(s): 05.40.−a, 46.70.Hg, 87.16.Dg, 05.10.−a

I. INTRODUCTION

The dominant repulsive force between layered chemical and biological systems, called membranes, is given by thermal out-of-plane fluctuations [1,2]. In the absence of tension, these membranes are called fluid and the fluctuations are controlled by the membranes' bending rigidity. There have been various theoretical approaches to compute the pressure of a single membrane between walls [1,3–7] or of a stack of membranes [1,3–5,8]. These situations are also interesting statistical mechanics problems.

Here we are concerned with the pressure generated by the bending fluctuations of a fluid membrane between two infinitely extended parallel walls, which has the form [1]

$$p=\alpha\frac{(k_BT)^2}{\kappa(d/2)^3}, \tag{1}$$

where κ is the bending rigidity of the membrane, d is the distance between the walls, and α is a factor that we wish to compute. Estimates of α have been ranging over the years from theoretical approximations $\alpha\approx 0.0242$ by Helfrich [1] and $\alpha\approx 0.0625$ by Janke and Kleinert, [3] through Monte Carlo estimates $\alpha=0.079\pm 0.002$ by Janke, Kleinert, and Meinhart [4] and $\alpha=0.0798\pm 0.0003$ by Gompper and Kroll [5] and a recent theoretical estimate $\alpha\approx 0.0797$ by Bachmann, Kleinert, and Pelster [7].

In Ref. [7], the result was obtained by replacing the hard walls by a $\tan^2$ potential, whose prefactor was sent to zero at the end of the calculation to recover hard walls. This corresponds to the strong-coupling limit $\alpha=\lim_{g\to\infty}\alpha(g)$ of a loop expansion of $\alpha(g)$, where $1/g^2$ is proportional to the prefactor of the potential. To achieve the necessary resummation, variational perturbation theory (VPT) [9] was used. This technique has been successful also in other situations where the strong-coupling limit of an asymptotic weak-coupling series is sought, e.g., when computing critical exponents from ϕ^4 field theory models [10]. In this work, we extend the four-loop calculation of Ref. [7] to five loops.

Our work is structured as follows. In Sec. II, we model the hard walls with two different potentials and give the perturbative results in Sec. III. In Sec. IV, we follow Ref. [7] and use VPT to estimate the strong-coupling limit corresponding to hard walls. In Sec. V, we consider the two different potentials to model the walls for a quantum mechanical (QM) particle in a box. The problem of finding the ground state energy for the QM problem is identical to computing the partition sum of a string between walls modeled by the same potential [6,11,12]. This problem in turn is structurally equivalent to finding $\alpha(g)$ in the membrane problem. Only for one of these potentials, the solution is known exactly [6,12]. Although the potentials are very similar in the region of interest, their behavior under resummation with VPT is rather different. This will be used to judge the quality of the results of using VPT for the membrane problem. In Sec. VI we force $\alpha(g)$ for the membrane problem to be identical to $\alpha(g)$ in the solvable QM problem by choosing the potential appropriately and extract α by determining the potential's singularities. In Sec. VII we discuss our results.

II. MODELING OF THE BOUNDARY CONDITIONS

Consider a tensionless membrane between two large flat parallel walls of area A separated by a distance d. In the harmonic approximation, which we are considering throughout, the curvature energy is given by

$$E=\frac{\kappa}{2}\int_A d^2x[\partial^2\varphi(\boldsymbol{x})]^2, \tag{2}$$

where κ is the membrane's bending rigidity and φ is a field that describes the membrane's position between the walls, which are located at $\pm d/2$. The d-dependent part f_d of the free energy density of the system at temperature T is given by the path integral

$$\exp\left(-\frac{Af_d}{k_BT}\right)=\prod_{\boldsymbol{x}}\int_{-d/2}^{+d/2}d\varphi(\boldsymbol{x})\exp\left(-\frac{E}{k_BT}\right). \tag{3}$$

The pressure is then obtained as

$$p=-\frac{\partial f_d}{\partial d} \tag{4}$$

and has the form (1) [1,3], and our task is to find the constant α.

*Email address: ka@physik.fu-berlin.de

The difficulty in computing the path integral (3) consists in implementing the restriction $-d/2<\varphi<d/2$. We follow Refs. [6,7] and add a potential term $m^4d^2\int d^2x V(\varphi/d)$ to E, where V has a sufficiently strong singularity at $\pm 1/2$, expand the potential V in a Taylor series in φ, and drop the restriction on φ. At the end of the calculation we take the limit $m\to 0$. We consider the potentials

$$V_c(z)=\frac{1}{2\pi^2\cos^2(\pi z)} \tag{5}$$

and

$$V_a(z)=\frac{1}{48}\left[\frac{1}{(1+2z)^2}+\frac{1}{(1-2z)^2}\right]. \tag{6}$$

The potentials have in common that they have quadratic divergences at $\pm 1/2$ and that their quadratic term in a Taylor expansion is normalized to $z^2/2$. V_c is related to the potential $V_t=(2\pi^2)^{-1}\tan^2(\pi x)$ used in Ref. [7] by $V_c=(2\pi^2)^{-1}+V_t$. For the resummation procedure employed in Ref. [7], V_c and V_t yield identical results and we will therefore recover the four-loop result reported there. For the other procedures used here, V_c is better suited than V_t.

Since the functional form of p in terms of κ, d, and T is known and since we are going to differentiate only with respect to d, we will set $k_BT=\kappa=1$ in the sequel. The energy functional may then be expanded as

$$E=\int d^2x\left\{\frac{1}{2}[\partial^2\varphi(\boldsymbol{x})]^2+\frac{1}{2}m^4\varphi(\boldsymbol{x})^2+m^4\epsilon_0 d^2 + m^4\sum_{k=2}^{\infty}\epsilon_{2k}d^{2(1-k)}\varphi(\boldsymbol{x})^{2k}\right\}, \tag{7}$$

where the ϵ_{2k} are the expansion coefficients of the potential.

The path integral can now be evaluated in a loop expansion [6,7]. The resulting Feynman diagrams, including their combinatorial factors, are obtained from recursion relations, whose derivation is delegated to Appendix A. The evaluation of the associated momentum integrals is detailed in Appendix C.

III. PERTURBATION THEORY

The diagrams labeled L-n (nth L-loop diagram) of Appendix A correspond apart from combinatorial factors $c_{L\text{-}n}$ and coupling constant factors $g_{L\text{-}n}$ to integrals in $\boldsymbol{x}$ space. Since the diagrams are connected and because of translational symmetry in the infinite-wall limit, we may split off a factor A from each diagram and represent the remainder in momentum space. A line represents then a propagator

$$\Delta(p^2,m^2)=\frac{1}{p^4+m^4}=\frac{i}{2m^2}\left(\frac{1}{p^2+im^2}-\frac{1}{p^2-im^2}\right), \tag{8}$$

while the integration measure over all independent momenta is

$$\int_p\equiv\int\frac{d^2p}{(2\pi)^2} \tag{9}$$

with momentum conservation at each vertex. A vertex with $2k$ legs represents a factor

$$-m^4d^{2(1-k)}\epsilon_{2k}. \tag{10}$$

The sum of all diagrams corresponds to the negative of the free energy density f_m, where the index refers to the presence of a nonzero m and $\lim_{m\to 0}f_m=f_d$.

In the sequel, a diagram represents only the corresponding momentum space integral which we call $I_{L\text{-}n}$, i.e., we split off not only a factor A, but also the combinatorial factor $c_{L\text{-}n}$ and the $-\epsilon_{2k}$ part of the factors (10), which we collect into $g_{L\text{-}n}$. Then f_m has L-loop expansions,

$$f_m=\frac{1}{d^2}\sum_{l=0}^{L}a_l g^{l-2}, \tag{11}$$

with

$$a_L=-\sum_n g_{L\text{-}n}c_{L\text{-}n}I_{L\text{-}n} \tag{12}$$

and a coupling constant

$$g=\frac{1}{m^2d^2}. \tag{13}$$

In Table III, we give $g_{L\text{-}n}$, $c_{L\text{-}n}$, and $I_{L\text{-}n}$ through five loops. For instance, the resulting zero-, one-, and two-loop contributions are

$$a_0=\epsilon_0,\qquad a_1=\frac{1}{8},\qquad a_2=\frac{3}{64}\epsilon_4. \tag{14}$$

Through five loops, we get for the potentials under consideration

L	a_L for V_c	a_L for V_a
0	0.0506606	0.0416667
1	0.125000	0.125000
2	0.154213	0.156250
3	0.105998	0.102307
4	0.026569	0.028101
5	−0.034229	−0.031426

(15)

IV. α FROM STRONG-COUPLING VARIATIONAL PERTURBATION THEORY

The d-dependent part of the free energy has for $m^2=0$ the form $f=4\alpha/d^2$, where the factor 4 ensures consistency with Eq. (1). Our task is to find an approximation to the strong-coupling limit $\alpha=\lim_{g\to\infty}\alpha(g)$ with L-loop expansions of $\alpha(g)$ given by

$$\alpha(g)=\frac{1}{4g^2}\sum_{l=0}^{L} a_l g^l, \tag{16}$$

with the knowledge of only the first few a_l. We will assume that $\alpha(g)$ has a strong-coupling expansion

$$\alpha(g)=\frac{1}{4}\sum_{m=0}^{\infty} a'_m g^{-2m/q} \tag{17}$$

with an additional parameter q. Then the problem has the following form: Given a function $f(g)=4\alpha(g)$ with L-loop weak-coupling expansions

$$f_L(g)=g^r\sum_{l=0}^{L} f_l^w g^l \tag{18}$$

and assuming strong-coupling expansions

$$f^M(g)=g^{p/q}\sum_{m=0}^{M} f_m^s g^{-2m/q}, \tag{19}$$

we are interested in finding f_0^s, p, and q. Assuming a thermodynamic limit for the problem at hand means setting $p=0$. Then α exists and is given by $\alpha=f_0^s/4$. In Ref. [7] it was additionally assumed that $q=1$, which is motivated by a similar QM problem, see Sec. V.

In VPT [9], we replace in Eq. (18),

$$\begin{aligned} g^{l+r}\to(tg)^{l+r}&\left\{\left(\frac{g}{\hat g}\right)^{2/q}+t\left[1-\left(\frac{g}{\hat g}\right)^{2/q}\right]\right\}^{[p-(l+r)q]/2}\\ &=\left(\frac{g}{\hat g}\right)^{p/q}(t\hat g)^{l+r}\left\{1+t\left[\left(\frac{\hat g}{g}\right)^{2/q}-1\right]\right\}^{[p-(l+r)q]/2}, \end{aligned} \tag{20}$$

reexpand the resulting expression in t through t^{L+r}, set $t=1$, and then optimize the resulting expression in $\hat g$, where optimizing refers to the principle of minimal sensitivity [13] and in practice means finding appropriate stationary or turning points. That is, we replace

$$g^{l+r}\to\left(\frac{g}{\hat g}\right)^{p/q}\hat g^{l+r}\sum_{k=0}^{L-l}\binom{[p-(l+r)q]/2}{k}\left[\left(\frac{\hat g}{g}\right)^{2/q}-1\right]^k \tag{21}$$

and optimize the resulting expression in $\hat g$. For V_c and V_a, where $r=-2$, we obtain with $p=0$,

$$\alpha_L=\frac{1}{4}\mathrm{opt}_{\hat g}\left[\sum_{l=0}^{L} a_l\hat g^{l-2}\sum_{k=0}^{L-l}\binom{(2-l)q/2}{k}(-1)^k\right] \tag{22}$$

as the L-loop variational approximation to α. This expression also holds for V_t, where $r=-1$. For $q=1$, the expression in square brackets is independent of a_0, which is why we reproduce below the results of Ref. [7].

If we do not want to make assumptions about q for f_m, we can determine it self-consistently by first treating $d\ln f_m^2/d\ln g$ in VPT, since it has the same q as f_m and since

$$\lim_{g\to\infty}\frac{d\ln f_m^2}{d\ln g}=\frac{p}{q} \tag{23}$$

with $p=0$ by assumption of a thermodynamic limit. That is, we resum the expansion of $d\ln f_m^2/d\ln g$ as detailed above and tune q such that optimization with respect to $\hat g$ leads to $d\ln f_m^2/d\ln g=0$.

A similar QM problem (see Sec. V below) leads us to try $q=1$. Let us consider the different potentials for modeling the walls that enclose the membrane with this assumption. The loop orders 0–2 do not admit a variational solution and we therefore take the perturbative results as our best approximation. Then the loop orders 0 and 1 yield zero for α, since they contain only negative powers of g, and the two-loop result is $\alpha_2=a_2/4$. The results through five loops are

L	α for V_c	α for V_a
2	0.038553	0.039063
3	0.073797	0.073688
4	0.079473	0.079422
5	0.081354	0.081345

(24)

with the results for V_c through four loops coinciding with those reported in Ref. [7]. An extrapolation of the results (24) suggests a value of α between 0.0820 and 0.0825.

The results from determining q self-consistently as described above are through five loops

	V_c		V_a	
L	q	α	q	α
3	0.38124	0.093076		
4	0.56789	0.095830	0.46463	0.098222
5	0.73907	0.090983	0.74209	0.090321

(25)

The values are compatible with convergence towards $q=1$ and with the α values for $q=1$, but convergence is too slow for any quantitative use.

V. QUANTUM MECHANICAL PARTICLE IN A BOX

A one-dimensional problem similar to the two-dimensional case above is finding the ground state energy of a QM particle in a one-dimensional box [12]. The Euclidean path integral to be computed is

$$\exp(-TE^{(0)})=\prod_t\int_{-d/2}^{+d/2} d\varphi(t)\exp(-E) \tag{26}$$

with

$$E=\frac{1}{2}\int_{-T/2}^{+T/2}dt\,\dot{\varphi}(t)^2, \tag{27}$$

where T is the total interaction time, being equivalent to the area A in the membrane case. In the large-T limit, $E^{(0)}$ is the ground state energy, for which we will test our approximation methods. Its exact value is

$$E^{(0)}=\frac{\pi^2}{2d^2}. \tag{28}$$

Again, we model the walls with a potential,

$$E=\int_{-T/2}^{+T/2}dt\left[\frac{1}{2}\dot{\varphi}(t)^2+m^2d^2V[\varphi(t)/d]\right], \tag{29}$$

and as in the membrane case for $f_m/(k_BT)$, we can write down a loop expansion for $E^{(0)}$. After modifying the Feynman rules according to

$$\frac{1}{p^4+m^4}\to\frac{1}{p^2+m^2},\quad \int\frac{d^2p}{(2\pi)^2}\to\int_{-\infty}^{+\infty}\frac{dp}{2\pi},$$
$$-m^4d^{2(1-k)}\epsilon_{2k}\to-m^2d^{2(1-k)}\epsilon_{2k} \tag{30}$$

and defining $\alpha(g)$ and g for the QM problem by

$$E^{(0)}=\frac{64\alpha(g)}{d^2},\qquad g=\frac{4}{md^2}, \tag{31}$$

not only can $\alpha(g)$ be expanded as in Eq. (16), but due to the simple relation (B5) between one-loop integrals in the membrane and QM cases, all diagrams that separate into one-loop integrals give the same contribution to $\alpha(g)$ in both cases [6]. It follows that for any given potential, a_0, a_1, and a_2, which involve at most one-loop topologies, are identical in the QM and the membrane problem.

For V_c, the exact ground state energy is known for any m and d [12],

$$E_c^{(0)}=\frac{\pi^2}{2d^2}\left(\frac{16}{\pi^4g^2}+\frac{1}{2}+\frac{4}{\pi^2g}\sqrt{1+\frac{\pi^4g^2}{64}}\right)$$
$$=\frac{\pi^2}{2d^2}\left(\frac{1}{2}+\frac{16}{\pi^4g^2}+\frac{1}{2}\sqrt{1+\frac{64}{\pi^4g^2}}\right). \tag{32}$$

The limiting value for $g\to\infty$ is in each case

$$\alpha=\frac{\pi^2}{128}\approx 0.077\,106\,3. \tag{33}$$

The coefficients a_l and a'_m in the weak- and strong-coupling expansions (16) and (17), respectively, can be obtained to arbitrary order simply by Taylor expanding Eq. (32). Note how this implies $q=1$ in VPT. This is the reason why we used $q=1$ in VPT for the membrane problem.

While for general potentials, the ground state energy cannot be computed exactly, it is possible to compute all Feynman diagrams analytically (see Appendix B). Alternatively, it is possible to compute the coefficients a_L to arbitrary order by generalizing [12] the Bender-Wu recursion relation for the anharmonic oscillator [14]. The generalized relation reads (correcting some typos in Eq. [12])

$$4jc_{nj}=2(j+1)(2j+1)c_{n,j+1}-\sum_{k=1}^{n}(-1)^k\epsilon_{2k+2}c_{n-k,j-k-1}$$
$$-2\sum_{k=1}^{n-1}c_{k1}c_{n-k,j},\qquad 1\leqslant j\leqslant 2n, \tag{34}$$

$c_{00}=1$, and $c_{nj}=0$ in all other cases. The a_L are then given by

$$a_L=\left(-\frac{1}{4}\right)^L c_{L-1,1},\qquad L\geqslant 2. \tag{35}$$

The results of carrying out VPT through 20 loops for the potentials V_c and V_a are collected in Table I and illustrated in Figs. 1 and 2. For fixed $q=1$ we get exponentially fast convergence towards the exact value of α for V_c. For V_a no convergence is obvious, although the values obtained through the order considered are not far from the exact α. Essentially the same is true when determining q self-consistently, except that the convergence towards the exact value of α is delayed as compared to taking $q=1$. For V_c, $q=1$ is approached exponentially fast, while for V_a, $q>1$ seems preferred at higher orders.

It is likely that the inferior convergence behavior for the potential V_a originates in our missing understanding of the analytical structure of $E^{(0)}$ as a function of g. It is possible that the strong-coupling behavior is not of the form (19) or that the strong-coupling expansion has a zero radius of convergence. Numerically, the deviations of the coefficients a_L from those for V_c are relatively small in low orders, in particular, the deviation from $a_L=0$ for small even $L>2$. Note how this is very similar to the results of the membrane loop expansion (15). Another likely similarity between the membrane problem and the QM problem with potential V_a is the factorial growth of a_L with L, for large L. In this respect, using V_c in the QM problem is very special, as already noted in Ref. [12], and it appears likely that the a_L grow factorially for the membrane problem for both V_c and V_a. Note, however, that the results for α with $q=1$ and also for α with self-consistently determined q improve with increasing L as long as the a_L do not significantly grow. We will come back to this point in Sec. VII.

VI. MEMBRANE PROBLEM WITH $\alpha(g)$ FROM PARTICLE IN A BOX

Let us compare the values for the QM expansion coefficients and the corresponding membrane coefficients using the potential V_c:

TABLE I. Determination of α (exact value $\alpha = 0.077\,106\,3\ldots$) for QM particle in a box through 20 loops. Values of α for both potentials with $q=1$ and values of q and α for both potentials with self-consistently determined q are shown.

	V_c				V_a			
		$q=1$	q self-cons.			$q=1$	q self-cons.	
L	a_L	α	q	α	a_L	α	q	α
0	0.0506606				0.0416667			
1	0.125				0.125			
2	0.154213	0.0385530			0.15625	0.0390625	0.309401	
3	0.0951261	0.0719411	0.605551	0.0836038	0.0911458	0.0717445	0.630222	0.0819600
4	0	0.0758821	0.850234	0.0807166	0.00325521	0.0758318	0.805894	0.0816667
5	−0.0361959	0.0767518	0.931591	0.0787187	−0.0340667	0.0767990	0.920850	0.0789522
6	0	0.0769910	0.966170	0.0778393	−0.012597	0.0770078	0.975808	0.0775787
7	0.0275454	0.0770659	0.982590	0.0774492	0.0421369	0.0770326	0.994979	0.0771334
8	0	0.0770913	0.990852	0.0772701	0.0400356	0.0770777	0.975795	0.0774386
9	−0.0262028	0.0771005	0.995143	0.0771857	−0.164914	0.0771337	0.957841	0.0778059
10	0	0.0771040	0.997410	0.0771451	−0.207989	0.0771252	1.000970	0.0771197
11	0.0279168	0.0771054	0.998617	0.0771254	1.56427	0.0770648	1.018330	0.0767930
12	0	0.0771059	0.999262	0.0771157	2.21468	0.0770447	1.008300	0.0769460
13	−0.0318674	0.0771061	0.999607	0.0771110	−25.1291	0.0771620	1.005830	0.0770638
14	0	0.0771062	0.999792	0.0771086	−43.0543	0.0771831	0.979132	0.0775060
15	0.0381093	0.0771063	0.999890	0.0771074	585.908	0.0771362	1.028460	0.0766838
16	0	0.0771063	0.999942	0.0771069	1288.21	0.0771241	1.038400	0.0765030
17	−0.0471274	0.0771063	0.999969	0.0771066	−18478.5	0.0771695	1.029930	0.0766691
18	0	0.0771063	0.999984	0.0771064	−53154.3	0.0772534	1.037170	0.0765617
19	0.0597739	0.0771063	0.999992	0.0771064	753376	0.0772069	1.024240	0.0768319
20	0	0.0771063	0.999996	0.0771063	2833593	0.0772520	1.051640	0.0762912

L	a_L^{QM}	a_L^{memb}	$a_L^{\mathrm{memb}} - a_L^{\mathrm{QM}}$
1	0.125	0.125	0
2	0.154213	0.154213	0
3	0.095126	0.105998	0.010872
4	0	0.026569	0.026569
5	−0.036196	−0.034229	0.001967

(36)

We see that the relative difference through the order considered is small when both a_L^{memb} and a_L^{QM} are nonzero. This is the motivation to carry out a different procedure for finding α from the loop expansion. Instead of asking directly what α is for a given potential for the membrane case, we slightly modify the ϵ_k order by order such that the expansion of $\alpha(g)$ is identical to that of the QM case with potential V_c and ask where the resulting potential has the nearest singularity. The scaling relation $f \propto 1/d^2$ when $m^2=0$ allows us then to recover α for the membrane case.

The expansion coefficients of the potentials are

	QM: V_c	Memb.
ϵ_0	0.0506606	0.0506606
ϵ_2	0.5	0.5
ϵ_4	3.28987	3.28987
ϵ_6	18.3995	18.0284
ϵ_8	94.6129	89.5702
ϵ_{10}	462.545	419.568

(37)

Let us instead investigate the expansion of

$$1/\sqrt{2\pi^2 V(x)} = \sum_{k=0}^{\infty} v_{2k} x^{2k}, \tag{38}$$

since for the QM case, we have $1/\sqrt{2\pi^2 V(x)} = \cos(\pi x)$. We can expect a good approximation for the location of the singularity of V if this singularity is of the quadratic type as in V_c and V_a. The expansion coefficients of the quantity (38) for the QM and membrane cases are

	QM	Memb.
v_0	1	1
v_2	−4.93480	−4.93480
v_4	4.05871	4.05871
v_6	−1.33526	2.32719
v_8	0.235331	−4.21557
v_{10}	−0.025807	−0.50636

(39)

The corresponding zeros x_0 of this function, corresponding to the singularity of $V(x)$, are

L	QM	Memb.
1	0.450158	0.450158
2	0.506893	0.506893
3	0.499717	0.523646
4	0.500008	0.514714
5	0.500000	0.514469

(40)

The value of α in each case is given by $(2x_0)^2$ times the exact value (33) of α for QM,

L	QM	Memb.
1	0.0625	0.0625
2	0.0792468	0.0792468
3	0.0770189	0.0845718
4	0.0771087	0.0817113
5	0.0771062	0.0816335

(41)

While the correct QM value (33) is approached very quickly, the convergence in the membrane case is slower. The fact that the last two values have such a small difference appears to be accidental. However, the results point towards a value above 0.080.

VII. SUMMARY AND DISCUSSION

We have used three methods to extract the pressure exerted by a tensionless membrane on two infinitely extended parallel walls from a five-loop calculation for smooth potentials. While variational perturbation theory with self-consistently determined q is converging too slowly for quantitative statements at five loops, variational perturbation theory with the assumption $q=1$ gives a result $\alpha \approx 0.0813$. The successive α values at the various loop orders in Eq. (24) suggest an extrapolated value of α between 0.0820 and 0.0825. Fixing $\alpha(g)$ to resemble the g structure of the ground state energy of a solvable quantum mechanics problem and analyzing the location of the singularities next to the origin of the resulting potential leads to $\alpha \approx 0.0816$. As opposed to the variational perturbation theory with $q=1$, the sequence given by the considered loop orders gives only a modest indication of where α might settle. The results of both analyses point towards a value above the Monte Carlo result $\alpha_{\mathrm{MC}}=0.0798\pm 0.0003$ [5].

We have also studied the quantum mechanics problem with a potential for which we do not know the exact solution but which is very close to the potential of the solvable problem in the region of interest. We have investigated both variational perturbation theory with self-consistently determined q and with $q=1$. The result is that the exponentially fast convergence of the solvable model towards the exact result for α cannot be expected for the general case, although good estimates of the exact result are obtained. Since numerically, this case is close to what happens in the membrane case, this gives us an indication on how trustworthy our results are. As already noted at the end of Sec. V, we can roughly state that the results for α in the quantum mechanics problem do not improve after the a_L start to significantly increase in magnitude. Along this reasoning, one may still expect improving the results for the membrane problem by proceeding to higher loop orders. In particular, going to six loops appears feasible with reasonable effort, since only eight of the 83 diagrams to be evaluated have no cutvertex and have therefore a true six-loop topology, as noted in Table II.

TABLE II. Numbers of vacuum diagrams for some low loop orders and numbers of those with full loop topology.

number of loops L	1	2	3	4	5	6	7
diagrams	1	1	3	7	24	83	376
diagrams with L-loop topology	1	0	1	1	5	8	37

ACKNOWLEDGMENT

The author is grateful to H. Kleinert for many useful discussions and for suggesting various resummation methods to extract α from the loop expansion.

APPENDIX A: RECURSION RELATION FOR THE LOOP EXPANSION

Here we define a loop expansion of the free energy and derive recursion relations for obtaining the required diagrams in a systematic way along the lines of Ref. [15]. We continue to work with $\kappa=k_BT=1$.

We write the energy functional (7) as

$$E[\varphi,G,\{L^{(2k)}\}]=\frac{1}{2}G_{12}^{-1}\varphi_1\varphi_2+L^{(0)}+\sum_{k=2}^{\infty}L^{(2k)}_{1,\ldots,2k}\varphi_1\cdots\varphi_{2k} \tag{A1}$$

with totally symmetric tensors G^{-1} and $L^{(2k)}$. Their indices $1,2,\ldots,2k$, are shorthands for space arguments $\boldsymbol{x}_1,\ldots,\boldsymbol{x}_{2k}$, and a generalized Einstein convention implies integration over space arguments that appear twice in a term. Comparison with Eq. (7) shows that

$$G_{12}^{-1}=\delta_{12}[\partial_1^2\partial_2^2+m^4] \tag{A2}$$

and

$$L^{(2k)}_{1,\ldots,2k}=m^4\epsilon_{2k}d^{2(1-k)}\delta_{1,\ldots,2k} \tag{A3}$$

with

$$\delta_{1,\ldots,2k}\equiv\int d^2x\,\delta(\boldsymbol{x}-\boldsymbol{x}_1)\cdots\delta(\boldsymbol{x}-\boldsymbol{x}_{2k}). \tag{A4}$$

Note that the index of ϵ_{2k} does not indicate a space argument and is exempted from the summation convention.

The free energy $Af_m=-W$ is given by

$$\exp(W[G,\{L^{(2k)}\}])=\int D\varphi\exp(-E[\varphi,G,\{L^{(2k)}\}]). \tag{A5}$$

W obeys the functional differential equation

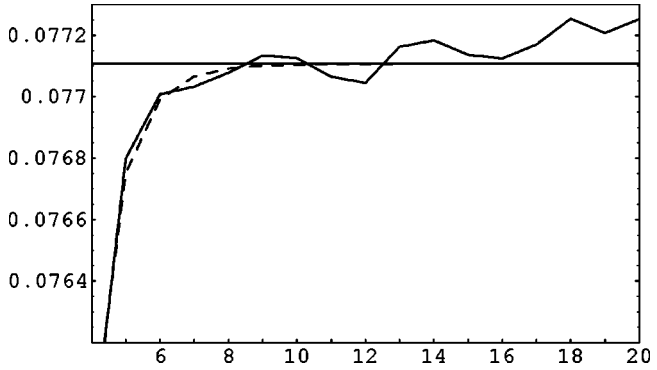

FIG. 1. Quantum mechanical particle in a box. α as a function of the loop order L for $q=1$ for V_c (dashed line), V_a (solid line) and the exact result (horizontal line). Note how the convergence towards the exact result is exponentially fast for V_t, while questionable for V_a.

$$0=\int D\varphi\,\frac{\delta}{\delta\varphi_1}\{\varphi_0\exp(-E[\varphi,G,\{L^{(2k)}\}])\}$$
$$=\left(\delta_{01}+2G_{12}^{-1}\frac{\delta}{\delta G_{02}^{-1}}-16L^{(4)}_{1234}\frac{\delta^2}{\delta G_{02}^{-1}\delta G_{34}^{-1}}\right.$$
$$\left.-4\sum_{k=3}^{\infty}kL^{(2k)}_{1,\ldots,2k}\frac{\delta^2}{\delta G_{02}^{-1}\delta L^{(2k-2)}_{3,\ldots,2k}}\right)\exp(W[G,\{L^{(2k)}\}]). \tag{A6}$$

Splitting $W\equiv W|_{L^{(2k)}=0}+W_I\equiv W_0+W_I$, so that W_0 obeys

$$\left(\delta_{01}+2G_{12}^{-1}\frac{\delta}{\delta G_{02}^{-1}}\right)\exp(W_0[G])=0, \tag{A7}$$

we get from Eq. (A6),

$$2G_{12}^{-1}\frac{\delta W_I}{\delta G_{12}^{-1}}-16L^{(4)}_{1234}\left(\frac{\delta^2 W}{\delta G_{12}^{-1}\delta G_{34}^{-1}}+\frac{\delta W}{\delta G_{12}^{-1}}\frac{\delta W}{\delta G_{34}^{-1}}\right)$$
$$-4\sum_{k=3}^{\infty}kL^{(2k)}_{1,\ldots,2k}\left(\frac{\delta^2 W}{\delta G_{12}^{-1}\delta L^{(2k-2)}_{3,\ldots,2k}}+\frac{\delta W}{\delta G_{12}^{-1}}\frac{\delta W}{\delta L^{(2k-2)}_{3,\ldots,2k}}\right)$$
$$=0, \tag{A8}$$

where we additionally have identified indices 0 and 1 and integrated over the respective variable. With

$$\frac{\delta W_0}{\delta G_{12}^{-1}}=-\frac{1}{2}G_{12} \tag{A9}$$

and

$$\frac{\delta^2 W_0}{\delta G_{12}^{-1}\delta G_{34}^{-1}}=\frac{1}{4}(G_{13}G_{24}+G_{14}G_{23}), \tag{A10}$$

Eq. (A8) may be transformed into

$$G_{12}\frac{\delta W_I}{\delta G_{12}}=-6L^{(4)}_{1234}G_{12}G_{34}-24L^{(4)}_{1234}G_{12}G_{35}G_{46}\frac{\delta W_I}{\delta G_{56}}$$
$$-8L^{(4)}_{1234}G_{15}G_{26}G_{37}G_{48}$$
$$\times\left(\frac{\delta^2 W_I}{\delta G_{56}\delta G_{78}}+\frac{\delta W_I}{\delta G_{56}}\frac{\delta W_I}{\delta G_{78}}\right)+\sum_{k=3}^{\infty}kL^{(2k)}_{1,\ldots,2k}$$
$$\times\left[G_{12}\frac{\delta W_I}{\delta L^{(2k-2)}_{3,\ldots,2k}}+2G_{1\bar{1}}\bar{G}_{2\bar{2}}\right.$$
$$\left.\times\left(\frac{\delta^2 W_I}{\delta G_{\bar{1}\bar{2}}\delta L^{(2k-2)}_{3,\ldots,2k}}+\frac{\delta W_I}{\delta G_{\bar{1}\bar{2}}}\frac{\delta W_I}{\delta L^{(2k-2)}_{3,\ldots,2k}}\right)\right. \tag{A11}$$

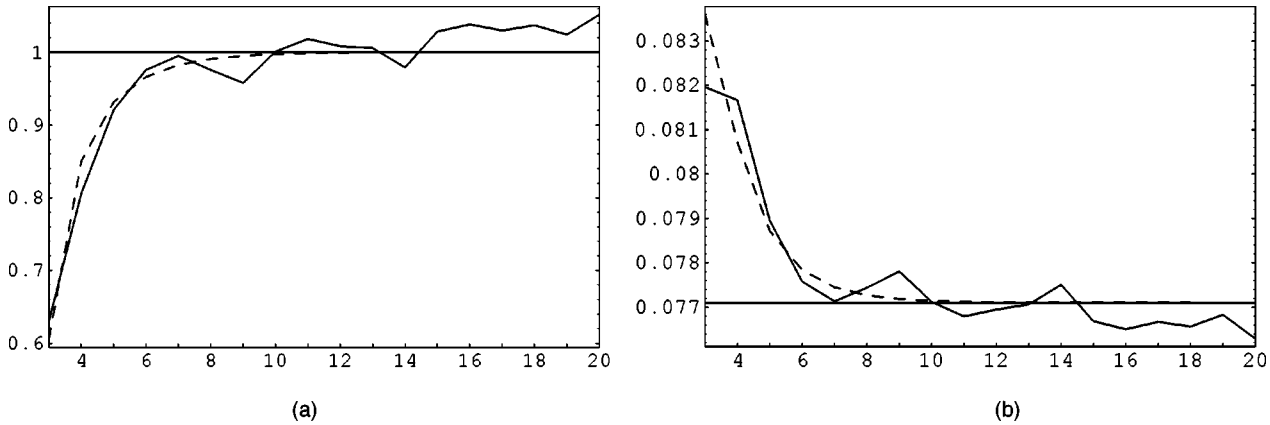

FIG. 2. Quantum mechanical particle in a box. (a) Self-consistently determined q as a function of the loop order L from V_c (dashed line), V_a (solid line) and $q=1$. Note how the convergence towards $q=1$ is exponentially fast for V_c, while for V_a, no convergence is obvious, although q is around 1. (b) α as a function of the loop order with self-consistently determined q for V_c (dashed line), V_a (solid line) and the exact result (horizontal line). Note how the convergence towards the exact result is exponentially fast for V_c, while questionable for V_a.

Consider a loop expansion,

$$W=\sum_{L=0}^{\infty} W^{(L)} \tag{A12}$$

and set

$$W^{(0)}=-\frac{A\epsilon_0}{d^2g^2} \tag{A13}$$

by an appropriate normalization of the path integral measure $D\varphi$. Then

$$W_0=W^{(1)}=-\frac{1}{2}\ln(G^{-1})_{11} \tag{A14}$$

and

$$W_I=\sum_{L=2}^{\infty} W^{(L)}. \tag{A15}$$

Equation (A11) separates into the two-loop equation

$$G_{12}\frac{\delta W^{(2)}}{\delta G_{12}}+6L^{(4)}_{1234}G_{12}G_{34}=0 \tag{A16}$$

and the recursion relation

$$\begin{aligned} G_{12}\frac{\delta W^{(L)}}{\delta G_{12}}=&-24L^{(4)}_{1234}G_{12}G_{35}G_{46}\frac{\delta W^{(L-1)}}{\delta G_{56}}\\ &-8L^{(4)}_{1234}G_{15}G_{26}G_{37}G_{48}\\ &\times\left(\frac{\delta^2 W^{(L-1)}}{\delta G_{56}\delta G_{78}}+\sum_{l=2}^{L-2}\frac{\delta W^{(l)}}{\delta G_{56}}\frac{\delta W^{(L-l)}}{\delta G_{78}}\right)\\ &+\sum_{k=3}^{L} kL^{(2k)}_{1,\ldots,2k}\left[G_{12}\frac{\delta W^{(L-1)}}{\delta L^{(2k-2)}_{3,\ldots,2k}}\right.\\ &+2G_{1\bar{1}}G_{2\bar{2}}\left(\frac{\delta^2 W^{(L-1)}}{\delta G_{\bar{1}\bar{2}}\delta L^{(2k-2)}_{3,\ldots,2k}}\right.\\ &\left.\left.+\sum_{l=2}^{L-k+1}\frac{\delta W^{(l)}}{\delta G_{\bar{1}\bar{2}}}\frac{\delta W^{(L-l)}}{\delta L^{(2k-2)}_{3,\ldots,2k}}\right)\right], \end{aligned} \tag{A17}$$

which holds for $L>2$ and where we have taken into account that a diagram containing the tensor $L^{(2k)}$ has at least k loops.

Equation (A16) is solved by

$$W^{(2)}=-3L^{(4)}_{1234}G_{12}G_{34}. \tag{A18}$$

Before carrying out the recursion relation (A17), let us introduce a graphical representation of the resulting terms. Represent each free propagator G_{12} by a line with two ends corresponding to the two space arguments $\boldsymbol{x}_1$ and $\boldsymbol{x}_2$ and each tensor $-L^{(n)}_{1,\ldots,n}$ by a dot. Each line end is connected to the dot with an identical space argument. Then a dot corresponding to a tensor $L^{(n)}_{1,\ldots,n}$ has n line ends connected to it. In this way all terms appearing in the $W^{(L)}$ with $L\neq 1$ can be graphically represented. The zero-loop order is represented by a dot without lines,

$$W^{(0)}=\bullet. \tag{A19}$$

Only $W^{(1)}$ does not fit into the graphical scheme above and as usual we use the graphical representation

$$W^{(1)}=\frac{1}{2}\ \bigcirc \tag{A20}$$

for it. Now we may write Eq. (A18) as

$$W^{(2)}=3\ \bigcirc\!\!\bullet\!\!\bigcirc \tag{A21}$$

which is the starting point for the recursive determination of the other $W^{(L)}$. For instance, the three-loop contribution to W is

$$W^{(3)}=12\ \bigcirc\!\!\!\bigcirc\ +36\ \bigcirc\!\!\bullet\!\!\bigcirc\!\!\bullet\!\!\bigcirc\ +15\ \bigcirc\!\!\bullet\!\!\bigcirc\ . \tag{A22}$$

In Table II we list the numbers of different diagrams through seven loops and the numbers of diagrams at each loop order which have no cutver tex (by definition, upon cutting through such a vertex appropriately, a diagram decomposes into two diagrams, which consequently have independent momentum integrations) and have therefore their full loop topology. The contributions through five loops for both the QM and the membrane problem are collected in Table III.

APPENDIX B: EVALUATION OF QUANTUM MECHANICAL INTEGRALS

All integrals in the QM case can be evaluated analytically. The propagator reads

$$\Delta(k^2,m^2)=\frac{1}{k^2+m^2}, \tag{B1}$$

its Fourier transform is

TABLE III. Diagrams L-n (nth L-loop diagram) through five loops and their combinatorial factors c_{L-n}, coupling constant factors g_{L-n}, and values I_{L-n} of the corresponding integrals for $m=1$. $D=1$ corresponds to the QM problem and $D=2$ to the membrane problem.

$L-n$	diagram	c_{L-n}	g_{L-n}	I_{L-n} for $D=1$	I_{L-n} for $D=2$
0-1	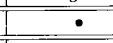	1	$-\epsilon_0$	1	1
1-1		1/2	1	$-J_0'=-1$	$-J_0'=-1/4$
2-1	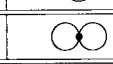	3	$-\epsilon_4$	1/4	$J_1^2=1/64$
3-1		12	ϵ_4^2	1/32	$\int_k \Delta_{\rm ol}^{(1,1)}(k^2,m^2)^2=4.04576\times10^{-4}$
3-2	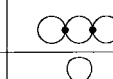	36	ϵ_4^2	1/16	$J_1^2J_2=1/1024$
3-3	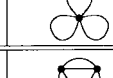	15	$-\epsilon_6$	1/8	$J_1^3=1/512$
4-1	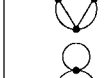	288	$-\epsilon_4^3$	3/512	$\int_k \Delta_{\rm ol}^{(1,1)}(k^2,m^2)^3=1.63237\times10^{-5}$
4-2	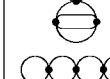	576	$-\epsilon_4^3$	5/512	$\frac{5}{8}J_1I_{3-1}=3.16075\times10^{-5}$
4-3	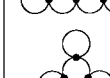	432	$-\epsilon_4^3$	1/64	$J_1^2J_2^2=1/16384$
4-4	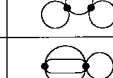	288	$-\epsilon_4^3$	3/128	$J_1^3J_3=3/32768$
4-5		360	$\epsilon_4\epsilon_6$	1/64	$J_1I_{3-1}=5.05719\times10^{-5}$
4-6	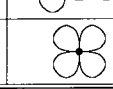	540	$\epsilon_4\epsilon_6$	1/32	$J_1^3J_2=1/8192$
4-7		105	$-\epsilon_8$	1/16	$J_1^4=1/4096$
5-1	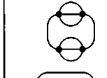	2592	ϵ_4^4	5/4096	$\int_k \Delta_{\rm ol}^{(1,1)}(k^2,m^2)^4=7.55133\times10^{-7}$
5-2	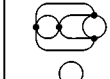	2304	ϵ_4^4	19/12288	$\int_k \Delta(k^2,m^2)^2\Delta_{ss}(k^2,m^2)^2=1.04187\times10^{-6}$
5-3	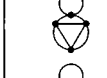	10368	ϵ_4^4	7/6144	$\int_k \Delta_{\rm ol}^{(1,1)}(k^2,m^2)\Delta_{\rm eye}(k^2,m^2)=6.71540\times10^{-7}$
5-4	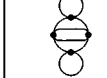	20736	ϵ_4^4	1/512	$\frac{2}{3}J_1I_{4-1}=1.36031\times10^{-6}$
5-5		10368	ϵ_4^4	13/4096	$J_1^2\int_k \Delta_{\rm ol}^{(1,2)}(k^2,m^2)^2=2.54723\times10^{-6}$
5-6	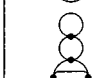	6912	ϵ_4^4	31/8192	$J_1^2\int_k \Delta(k^2,m^2)^3\Delta_{ss}(k^2,m^2)=3.09329\times10^{-6}$
5-7	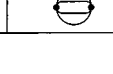	6912	ϵ_4^4	5/2048	$\frac{5}{8}J_1J_2I_{3-1}=1.97547\times10^{-6}$
5-8	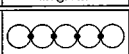	5184	ϵ_4^4	1/256	$J_1^2J_2^3=1/262144$
5-9	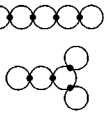	10368	ϵ_4^4	3/512	$J_1^3J_2J_3=3/524288$
5-10	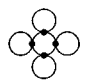	2592	ϵ_4^4	5/512	$J_1^4J_4=5/524288$
5-11		5760	$-\epsilon_4^2\epsilon_6$	7/3072	$\int_k \Delta(k^2,m^2)\Delta_{ss}(k^2,m^2)^2=1.50770\times10^{-6}$
5-12	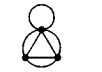	12960	$-\epsilon_4^2\epsilon_6$	3/1024	$J_1I_{4-1}=2.04047\times10^{-6}$
5-13		4320	$-\epsilon_4^2\epsilon_6$	5/1024	$\frac{5}{8}J_1^2I_{3-1}=3.95093\times10^{-6}$
5-14	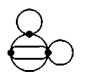	17280	$-\epsilon_4^2\epsilon_6$	5/1024	$\frac{5}{8}J_1^2I_{3-1}=3.95093\times10^{-6}$
5-15	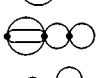	4320	$-\epsilon_4^2\epsilon_6$	1/256	$J_1J_2I_{3-1}=3.16075\times10^{-6}$
5-16	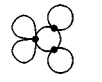	6480	$-\epsilon_4^2\epsilon_6$	3/256	$J_1^4J_3=3/262144$
5-17	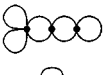	6480	$-\epsilon_4^2\epsilon_6$	1/128	$J_1^3J_2^2=1/131072$
5-18	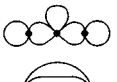	6480	$-\epsilon_4^2\epsilon_6$	1/128	$J_1^3J_2^2=1/131072$
5-19	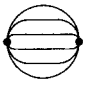	360	ϵ_6^2	1/192	$\int_k \Delta_{ss}(k^2,m^2)^2=3.76084\times10^{-6}$
5-20	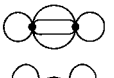	2700	ϵ_6^2	1/128	$J_1^2I_{3-1}=6.32149\times10^{-6}$
5-21	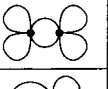	2025	ϵ_6^2	1/64	$J_1^4J_2=1/65536$
5-22	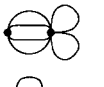	5040	$\epsilon_4\epsilon_8$	1/128	$J_1^2I_{3-1}=6.32149\times10^{-6}$
5-23	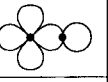	5040	$\epsilon_4\epsilon_8$	1/64	$J_1^4J_2=1/65536$
5-24	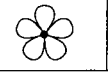	945	$-\epsilon_{10}$	1/32	$J_1^5=1/32768$

$$\tilde{\Delta}(t,m)=\int_{-\infty}^{+\infty}\frac{dk}{2\pi}\frac{e^{ikt}}{k^2+m^2}=\frac{e^{-m|t|}}{2m}. \tag{B2}$$

For most integrals it is convenient to work in t space, omitting the last t integration (which, due to time translation invariance, gives a factor T, the total interaction time). An exception are the one-loop integrals, which are computed easiest in momentum space. Using dimensional regularization, we get

$$\begin{aligned} J_0' &= \int \frac{d^Dp}{(2\pi)^D}\ln(p^2+m^2)\bigg|_{D=1} \\ &= -\frac{1}{D}\int \frac{d^Dp}{(2\pi)^D}p_\mu\frac{\partial}{\partial_\mu}\ln(p^2+m^2)\bigg|_{D=1} \\ &= -\frac{2}{D}\int \frac{d^Dp}{(2\pi)^D}\frac{p^2}{p^2+m^2}\bigg|_{D=1}=m \end{aligned} \tag{B3}$$

for the only diverging integral, while the other one-loop integrals are given by

$$J_n \equiv \int_{-\infty}^{+\infty} \frac{dp}{2\pi} \frac{1}{(p^2+m^2)^n} = \frac{m^{1-2n}}{2} \frac{\Gamma\left(n-\frac{1}{2}\right)}{\sqrt{\pi}\Gamma(n)}. \quad \text{(B4)}$$

Note the similarity to the membrane one-loop integrals (C1) and (C2) below, so that

$$J_0'^{\mathrm{qm}} = 4m^{-1} J_0'^{\mathrm{memb}}, \qquad J_n^{\mathrm{qm}} = 4m^{2n-1} J_n^{\mathrm{memb}}. \quad \text{(B5)}$$

APPENDIX C: EVALUATION OF MEMBRANE INTEGRALS

In the following, we will always assume that $m^2 > 0$. We give results in a form suited for numerical integration of the remaining loop momenta.

1. One-loop vacuum integrals

The ubiquitous one-loop integrals without external momenta can be computed analytically as

$$J_0' \equiv \int \frac{d^D p}{(2\pi)^D} \ln(p^4+m^4)\bigg|_{D=2} = -\frac{1}{D}\int \frac{d^D p}{(2\pi)^D} p_\mu \frac{\partial}{\partial_\mu} \ln(p^4+m^4)\bigg|_{D=2} = -\frac{4}{D}\int \frac{d^D p}{(2\pi)^D} \frac{p^4}{p^4+m^4}\bigg|_{D=2} = \frac{m^2}{4} \quad \text{(C1)}$$

and

$$J_n \equiv \int_p \frac{1}{(p^4+m^4)^n} = \frac{m^{2-4n}}{8} \frac{\Gamma\left(n-\frac{1}{2}\right)}{\sqrt{\pi}\Gamma(n)}, \quad \text{(C2)}$$

where dimensional regularization has been employed for J_0'.

2. One-loop bubble

Several diagrams contain the one-loop bubble

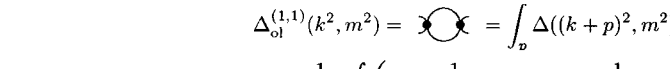

$$\begin{aligned}
\Delta_{\mathrm{ol}}^{(1,1)}(k^2,m^2) &= \int_p \Delta((k+p)^2,m^2)\Delta(p^2,m^2) \\
&= -\frac{1}{4m^4}\int_p \left(\frac{1}{(k+p)^2+im^2} - \frac{1}{(k+p)^2-im^2}\right)\left(\frac{1}{p^2+im^2} - \frac{1}{p^2-im^2}\right) \\
&= -\frac{1}{4m^4}\left[\psi_{\mathrm{ol}}^{(1,1)}(k^2,m^2,m^2) - \psi_{\mathrm{ol}}^{(1,1)}(k^2,m^2,-m^2) - \psi_{\mathrm{ol}}^{(1,1)}(k^2,-m^2,m^2) + \psi_{\mathrm{ol}}^{(1,1)}(k^2,-m^2,-m^2)\right]
\end{aligned} \quad \text{(C3)}$$

with $\psi_{\mathrm{ol}}^{(1,1)}$ defined by

$$\psi_{\mathrm{ol}}^{(1,1)}(k^2,m_1^2,m_2^2) \equiv \int_p \frac{1}{[(p+k)^2+im_1^2](p^2+im_2^2)}. \quad \text{(C4)}$$

Elementary integration gives

$$\psi_{\mathrm{ol}}^{(1,1)}(k^2,\pm m^2,\pm m^2) = \frac{1}{2\pi\sqrt{k^2}\sqrt{k^2\pm 4im^2}} \ln \frac{\sqrt{k^2\pm 4im^2}+\sqrt{k^2}}{\sqrt{k^2\pm 4im^2}-\sqrt{k^2}} \quad \text{(C5)}$$

and

$$\psi_{\mathrm{ol}}^{(1,1)}(k^2,\pm m^2,\mp m^2) = \frac{1}{4\pi\sqrt{k^4-4m^4}} \ln \frac{k^2+\sqrt{k^4-4m^4}}{k^2-\sqrt{k^4-4m^4}}, \quad \text{(C6)}$$

so that

$$\Delta_{\mathrm{ol}}^{(1,1)}(k^2,m^2) = \frac{1}{8\pi m^4}\left[\frac{1}{\sqrt{k^4-4m^4}} \ln \frac{k^2+\sqrt{k^4-4m^4}}{k^2-\sqrt{k^4-4m^4}} - 2\mathrm{Re}\left(\frac{1}{\sqrt{k^2}\sqrt{k^2-4im^2}} \ln \frac{\sqrt{k^2-4im^2}+\sqrt{k^2}}{\sqrt{k^2-4im^2}-\sqrt{k^2}}\right)\right]. \quad \text{(C7)}$$

Now we can also easily compute

$$\Delta_{\rm ol}^{(1,2)}(k^2,m^2) = \quad = \int_p \Delta((k+p)^2,m^2)\Delta(p^2,m^2)^2 = -\frac{1}{4m^2}\frac{\partial}{\partial m^2}\Delta_{\rm ol}^{(1,1)}(k^2,m^2)$$
$$= \frac{5k^2}{4\pi m^4(k^4-4m^4)(k^4+16m^4)}$$
$$+\frac{1}{16\pi m^8}\left[\frac{k^4-6m^4}{(k^4-4m^4)^{3/2}}\ln\frac{k^2+\sqrt{k^4-4m^4}}{k^2-\sqrt{k^4-4m^4}} - 2\mathrm{Re}\left(\frac{k^2+5im^2}{\sqrt{k^2}(k^2+4im^2)^{3/2}}\ln\frac{\sqrt{k^2+4im^2}+\sqrt{k^2}}{\sqrt{k^2+4im^2}-\sqrt{k^2}}\right)\right]. \tag{C8}$$

3. Sunset self-energy

For several diagrams we need to compute

$$\Delta_{\rm ss}(k^2,m^2) = \quad = \int_{pq}\Delta((k+p)^2,m^2)\Delta((p+q)^2,m^2)\Delta(q^2,m^2)$$
$$= -\frac{i}{8m^6}\left[\psi_{\rm ss}(k^2,m^2,m^2,m^2)-\psi_{\rm ss}(k^2,m^2,m^2,-m^2)-\psi_{\rm ss}(k^2,m^2,-m^2,m^2)+\psi_{\rm ss}(k^2,m^2,-m^2,-m^2)\right.$$
$$\left.-\psi_{\rm ss}(k^2,-m^2,m^2,m^2)+\psi_{\rm ss}(k^2,-m^2,m^2,-m^2)+\psi_{\rm ss}(k^2,-m^2,-m^2,m^2)-\psi_{\rm ss}(k^2,-m^2,-m^2,-m^2)\right] \tag{C9}$$

with $\psi_{\rm ss}$ defined by

$$\psi_{\rm ss}(k^2,m_1^2,m_2^2,m_3^2)\equiv\int_{pq}\frac{1}{[(k+p)^2+im_1^2][(p+q)^2+im_2^2](q^2+im_3^2)}. \tag{C10}$$

Note that

$$\psi_{\rm ss}(k^2,m^2,m^2,m^2)=\psi_{\rm ss}(k^2,-m^2,-m^2,-m^2)^* \tag{C11}$$

and

$$\psi_{\rm ss}(k^2,-m^2,m^2,m^2)=\psi_{\rm ss}(k^2,m^2,-m^2,m^2)=\psi_{\rm ss}(k^2,m^2,m^2,-m^2)=\psi_{\rm ss}(k^2,m^2,-m^2,-m^2)^*=\psi_{\rm ss}(k^2,-m^2,m^2,-m^2)^*$$
$$=\psi_{\rm ss}(k^2,-m^2,-m^2,m^2)^*. \tag{C12}$$

$\psi_{\rm ss}$ may be evaluated as

$$\psi_{\rm ss}(k^2,m_1^2,m_2^2,m_3^2)=\int_0^1 d\alpha\int_p\frac{1}{(k+p)^2+im_1^2}\int_q\frac{1}{[q^2+2\alpha pq+\alpha p^2+\alpha im_2^2+(1-\alpha)im_3^2]^2}$$
$$=\frac{1}{4\pi}\int_0^1 d\alpha\int_p\frac{1}{[(k+p)^2+im_1^2][\alpha(1-\alpha)p^2+\alpha im_2^2+(1-\alpha)im_3^2]}$$
$$=\frac{1}{4\pi}\int_0^1\frac{d\alpha}{\alpha(1-\alpha)}\int_0^1 d\beta\int_p\frac{1}{\left[p^2+2(1-\beta)pk(1-\beta)(k^2+im_1^2)+\beta i\left(\frac{m_2^2}{1-\alpha}+\frac{m_3^2}{\alpha}\right)\right]^2}$$
$$=\frac{1}{(4\pi)^2}\int_0^1\frac{d\alpha}{\alpha(1-\alpha)}\int_0^1 d\beta\frac{1}{\beta(1-\beta)k^2+(1-\beta)im_1^2+\beta i\left(\frac{m_2^2}{1-\alpha}+\frac{m_3^2}{\alpha}\right)}$$
$$=\frac{1}{(4\pi)^2}\int_0^1 d\alpha\int_0^1 d\beta\frac{1}{\alpha(1-\alpha)(1-\beta)(\beta k^2+im_1^2)+\beta i[\alpha m_2^2+(1-\alpha)m_3^2]}$$
$$=\frac{2}{(4\pi)^2}\int_0^1 d\beta\int_{-1}^{+1}dx\frac{1}{(1-x^2)(1-\beta)(\beta k^2+im_1^2)+2i\beta[(1+x)m_2^2+(1-x)m_3^2]}. \tag{C13}$$

If $m_3^2=m_2^2$, this becomes

$$\psi_{\rm ss}(k^2,m_1^2,m_2^2,m_2^2)=\frac{2}{(4\pi)^2}\int_0^1 d\beta\int_{-1}^{+1}dx\frac{1}{(1-x^2)(1-\beta)(\beta k^2+im_1^2)+4i\beta m_2^2},$$
$$=\frac{2}{(4\pi)^2}\int_0^1\frac{d\beta}{(1-\beta)(\beta k^2+im_1^2)}\int_{-1}^{+1}dx\,\frac{1}{1+\dfrac{4i\beta m_2^2}{(1-\beta)(\beta k^2+im_1^2)}-x^2}, \tag{C14}$$

while for $m_3^2=-m_2^2$ we have

$$\psi_{\rm ss}(k^2,m_1^2,m_2^2,-m_2^2)=\frac{2}{(4\pi)^2}\int_0^1 d\beta\int_{-1}^{+1}dx\frac{1}{(1-x^2)(1-\beta)(\beta k^2+im_1^2)+4ix\beta m_2^2},$$
$$=\frac{2}{(4\pi)^2}\int_0^1\frac{d\beta}{(1-\beta)(\beta k^2+im_1^2)}\int_{-1}^{+1}dx\frac{1}{1-x^2+\dfrac{4i\beta m_2^2}{(1-\beta)(\beta k^2+im_1^2)}x}. \tag{C15}$$

Noting that the formulas

$$f_1(z)=\int_{-1}^{+1}\frac{dx}{z-x^2}=\frac{1}{2\sqrt{z}}\int_{-1}^{+1}dx\left(\frac{1}{\sqrt{z}+x}+\frac{1}{\sqrt{z}-x}\right)=\frac{\ln(\sqrt{z}+1)-\ln(\sqrt{z}-1)}{\sqrt{z}} \tag{C16}$$

and

$$f_2(z)\equiv\int_{-1}^{+1}\frac{dx}{1-x^2+2zx}=\frac{1}{2\sqrt{1+z^2}}\int_{-1}^{+1}dx\left(\frac{1}{\sqrt{1+z^2}-z+x}+\frac{1}{\sqrt{1+z^2}+z-x}\right)=\frac{1}{2\sqrt{1+z^2}}[\ln(\sqrt{1+z^2}-z+1)$$
$$-\ln(\sqrt{1+z^2}-z-1)-\ln(\sqrt{1+z^2}+z-1)+\ln(\sqrt{1+z^2}+z+1)] \tag{C17}$$

are numerically safe to use if the branch cut of the logarithm is taken from 0 to $-\infty$, we may now express the $\psi_{\rm ss}$ in Eq. (C9) with the help of β integrals involving f_1 and f_2. However, these integrals are difficult to evaluate numerically if $m_3^2=m_2^2=-m_1^2$. These cases may be avoided by making use of Eq. (C12). Together with Eq. (C11) we get

$$\Delta_{\rm ss}(k^2,m^2)=\frac{1}{8m^6}{\rm Im}[2\psi_{\rm ss}(k^2,m^2,m^2,m^2)-6\psi_{\rm ss}(k^2,m^2,m^2,-m^2)]=\frac{1}{32\pi^2m^6}{\rm Im}\int_0^1\frac{d\beta}{(1-\beta)(\beta k^2+im^2)}$$
$$\times\left[f_1\left(1+\frac{4i\beta m^2}{(1-\beta)(\beta k^2+im^2)}\right)-3f_2\left(\frac{2i\beta m^2}{(1-\beta)(\beta k^2+im^2)}\right)\right]. \tag{C18}$$

This form is easy to implement numerically.

4. Eye bubble and triangle coupling

For the integral $I_{5\text{-}3}$, we need the eye bubble subdiagram

$\Delta_{\rm eye}(k^2,m^2)$ =  $=\int_r\Delta_{\rm tr}(k,r,m^2)^2,$ (C19)

where the triangle subdiagram $\Delta_{\rm tr}$ is given by

$$\Delta_{\rm tr}(k,r,m^2) = \quad = \int_p \Delta(p^2,m^2)\Delta((p+k)^2,m^2)\Delta((p+r)^2,m^2)$$
$$= -\frac{i}{8(2\pi)^2 m^6}\left[\psi_{\rm tr}(k,r,m^2,m^2,m^2) - \psi_{\rm tr}(k,r,m^2,m^2,-m^2)\right.$$
$$- \psi_{\rm tr}(k,r,m^2,-m^2,m^2) + \psi_{\rm tr}(k,r,m^2,-m^2,-m^2)$$
$$- \psi_{\rm tr}(k,r,-m^2,m^2,m^2) + \psi_{\rm tr}(k,r,-m^2,m^2,-m^2)$$
$$\left. + \psi_{\rm tr}(k,r,-m^2,-m^2,m^2) - \psi_{\rm tr}(k,r,-m^2,-m^2,-m^2)\right]$$
$$= \frac{1}{(4\pi)^2 m^6}\,{\rm Im}\left[\psi_{\rm tr}(k,r,m^2,m^2,m^2) - \psi_{\rm tr}(k,r,m^2,m^2,-m^2)\right.$$
$$\left. - \psi_{\rm tr}(k,r,m^2,-m^2,m^2) + \psi_{\rm tr}(k,r,m^2,-m^2,-m^2)\right] \tag{C20}$$

with $\psi_{\rm tr}$ defined by

$$\psi_{\rm tr}(k,r,m_1^2,m_2^2,m_3^2) \equiv \int \frac{d^2p}{(p^2+im_1^2)[(p+k)^2+im_2^2][(p+r)^2+im_3^2]}$$
$$= \int_0^\infty dp\,p \int_0^{2\pi} d\phi \frac{1}{(p^2+im_1^2)[p^2+k^2+2pk\cos(\phi-\phi_k)+im_2^2][p^2+r^2+2pr\cos(\phi-\phi_r)+im_3^2]}$$
$$= \int_0^{2\pi} d\phi \int_0^\infty \frac{dp\,p}{(p-a_+)(p-a_-)(p-b_+)(p-b_-)(p-c_+)(p-c_-)}$$
$$= -\int_0^{2\pi} d\phi \left\{ \frac{1}{a_+-a_-}\left[\frac{a_+\ln a_+}{(a_+-b_+)(a_+-b_-)(a_+-c_+)(a_+-c_-)}\right.\right.$$
$$\left. - \frac{a_-\ln a_-}{(a_--b_+)(a_--b_-)(a_--c_+)(a_--c_-)}\right] + \frac{1}{b_+-b_-}\left[\frac{b_+\ln b_+}{(b_+-a_+)(b_+-a_-)(b_+-c_+)(b_+-c_-)}\right.$$
$$\left. - \frac{b_-\ln b_-}{(b_--a_+)(b_--a_-)(b_--c_+)(b_--c_-)}\right] + \frac{1}{c_+-c_-}\left[\frac{c_+\ln c_+}{(c_+-a_+)(c_+-a_-)(c_+-b_+)(c_+-b_-)}\right.$$
$$\left.\left. - \frac{c_-\ln c_-}{(c_--a_+)(c_--a_-)(c_--b_+)(c_--b_-)}\right]\right\}, \tag{C21}$$

with

$$a_\pm = \pm i\sqrt{im_1^2}, \tag{C22}$$

$$b_\pm = -k\cos(\phi-\phi_k) \pm i\sqrt{k^2\sin^2(\phi-\phi_k)+im_2^2}, \tag{C23}$$

$$c_\pm = -r\cos(\phi-\phi_r) \pm i\sqrt{r^2\sin^2(\phi-\phi_r)+im_3^2}. \tag{C24}$$

For the numerical evaluation of $I_{5\text{-}3}$, it is also useful to know the large-k behavior

$$\Delta_{\rm eye}(k^2,m^2) = \frac{2}{k^8} I_{3\text{-}1}, \quad k^2 \gg m^2 \tag{C25}$$

with $I_{3\text{-}1}$ from Table III.

Let us remark here that $\psi_{\rm tr}$ and therefore $\Delta_{\rm tr}$ can also be computed analytically (e.g., by performing the integrals over the Cartesian components p_x and p_y of p), but the resulting expressions are rather lengthy and it may be a delicate issue to remain on the same Riemann sheet while evaluating the logarithms and square roots involved.

5. Numerical considerations

Most integrals are evaluated rather easily. They are either known analytically, involve only one numeric integration, or involve one such integration involving the function $\Delta_{\rm ss}(k^2,m^2)$, whose evaluation implies one numeric integration, see Eq. (C18). These cases are easily dealt with by using any standard software integration package, e.g., MATHEMATICA, which was used here. A lot of integrals can be evaluated in different ways, so the safety of using

$\Delta_{ss}(k^2,m^2)$ inside an integral can be and has been checked. For instance, the integral $I_{3\text{-}1}$ can be performed by integrating either $\Delta_{ol}^{(1,1)}(k^2,m^2)^2$ or $\Delta_{ss}(k^2,m^2)\Delta(k^2,m^2)$ over k^2. By such cross checks and by varying the settings within MATHEMATICA for the numerical integrations, one may easily gain confidence that the integrations performed are accurate through the number of digits given in Table III.

The only exception to the above considerations through five loops is integral $I_{5\text{-}3}$. As indicated in Table III, the product $\Delta_{ol}^{(1,1)}(k^2,m^2)\Delta_{eye}(k^2,m^2)$ has to be integrated over k^2. While $\Delta_{ol}^{(1,1)}(k^2,m^2)$ is known analytically from Eq. (C7), $\Delta_{eye}(k^2,m^2)$ involves a further two-dimensional numeric integration of $\Delta_{tr}(k,r,m^2)^2$ over r, see Eq. (C19). $\Delta_{tr}(k,r,m^2)$ itself implies a one-dimensional numeric integration, see Eqs. (C20) and (C21). Using this method, an uncertainty in the last digit given in Table III remained in our computations. We achieved the precision through the last digit given in Table III by rewriting $I_{5\text{-}3}$ as the five-dimensional integral

$$I_{5\text{-}3}=\frac{1}{2^7\pi^5}\int_0^\infty dp^2\int_0^\infty dq^2\int_0^\infty dr^2\int_0^\pi d\phi_{pr}\int_0^{2\pi}d\phi_{qr}\times\Delta(p^2,m^2)\Delta(q^2,m^2)\Delta([p+r]^2,m^2)\Delta([q+r]^2,m^2)\Delta_{ol}^{(1,1)}(r^2,m^2)\Delta_{ol}^{(1,1)}([p-q]^2,m^2) \quad \text{(C26)}$$

in an obvious notation and using MATHEMATICA for successively increasing precisions of the final result.

The precision achieved for all integrals is several orders of magnitude better than needed to determine, say, the first three nonzero digits of our estimates for α. Higher precision is easily attained for all integrals but $I_{5\text{-}3}$, but is unnecessary for the purpose of this work.

[1] W. Helfrich, Z. Naturforsch. **33A**, 305 (1978); W. Helfrich and M. Servuss, Nuovo Cimento D **3**, 137 (1984).

[2] I. Bivas and A.G. Petrov, J. Theor. Biol. **88**, 4591 (1981); D. Sornette and N. Ostrowski, J. Phys. (Paris) **45**, 265 (1984).

[3] W. Janke and H. Kleinert, Phys. Lett. A **117**, 353 (1986).

[4] W. Janke, H. Kleinert, and M. Meinhart, Phys. Lett. B **217**, 525 (1989).

[5] G. Gompper and D.M. Kroll, Europhys. Lett. **9**, 59 (1989).

[6] H. Kleinert, Phys. Lett. A **257**, 269 (1999).

[7] M. Bachmann, H. Kleinert, and A. Pelster, Phys. Lett. A **261**, 127 (1999).

[8] W. Janke and H. Kleinert, Phys. Rev. Lett. **58**, 144 (1987); F. David, J. Phys. (France) **51**, C7-115 (1990); R.R. Netz and R. Lipowski, Europhys. Lett. **29**, 345 (1995); M. Bachmann, H. Kleinert, and A. Pelster, Phys. Rev. E **63**, 051709 (2001).

[9] H. Kleinert, *Path Integrals in Quantum Mechanics, Statistics and Polymer Physics*, 2nd ed. (World Scientific, Singapore, 1995), Chap. 5.

[10] H. Kleinert and V. Schulte-Frohlinde, *Critical Properties of ϕ^4-Theories*, 1st ed. (World Scientific, Singapore, 2001), Chap.19.

[11] P.-G. de Gennes, J. Chem. Phys. **48**, 2257 (1968); R. Lipowski, Z. Phys. B Condens. Matter **97**, 193 (1995); C. Hiergeist and R. Lipowski, Physica A **244**, 164 (1997).

[12] H. Kleinert, A. Chervyakov, and B. Hamprecht, Phys. Lett. A **260**, 182 (1999).

[13] P.M. Stevenson, Phys. Rev. D **23**, 2916 (1981).

[14] C.M. Bender and T.T. Wu, Phys. Rev. **184**, 1231 (1969); Phys. Rev. D **7**, 1620 (1973).

[15] B. Kastening, Phys. Rev. E **61**, 3501 (2000); H. Kleinert, A. Pelster, B. Kastening, and M. Bachmann, *ibid.* **62**, 1537 (2000); H. Kleinert and A. Pelster, e-print hep-th/0006153.